

IMAGING STRATEGY

## Comparison of ECG-Gated Rectilinear vs. Real-Time Radial K-Space Sampling Schemes in Cine True-FISP Cardiac MRI

Daniel T. Boll,<sup>1</sup> Elmar M. Merkle,<sup>1</sup> Danielle M. Seaman,<sup>1</sup>  
Robert C. Gilkeson,<sup>1</sup> Andrew P. Larson,<sup>2</sup> Orlando P. Simonetti,<sup>2</sup>  
Jeffrey L. Duerk,<sup>1</sup> and Jonathan S. Lewin, M.D.<sup>1,\*</sup>

<sup>1</sup>Department of Radiology, University Hospitals of Cleveland Case Western Reserve University, Cleveland, Ohio, USA

<sup>2</sup>Cardiovascular MR Research Group, Siemens Medical Solutions, Chicago, Illinois, USA

### ABSTRACT

*Purpose.* To compare three k-space sampling schemes in cine True-FISP cardiac magnetic resonance imaging and to evaluate changes in calculated quantitative functional cardiac parameters as a function of underlying k-space sampling techniques. *Material and Methods.* Using a 1.5 T MR imaging system (Magnetom Sonata, Siemens Medical Solutions, Erlangen, Germany), three k-space data-sampling schemes: rectilinear (2.96 ms/1.58 ms/70°/12 s TR/TE/FA/AcquisitionTime), and two radial k-space acquisitions, with filtered back-projection (RADIAL) (2.45 ms/1.25 ms/50°/3.3 s TR/TE/FA/AT), and steady-state projection imaging with dynamic echo-train readout (SPIDER) (3.39 ms/1.62 ms/55°/1.8 s TR/TE/FA/AT) of a True-FISP sequence were applied in 10 healthy volunteers. Long- and short-axis breath-hold series were acquired and signal-to-noise ratios (SNR) for blood and myocardium were determined, as was contrast-to-noise ratios (CNR). Quantitative cardiac functional analysis included: determination of end-systolic/end-diastolic volumes, ejection fraction, and left ventricular mass. Functional analysis was performed by two independent readers three times for each volunteer and k-space sampling strategy. Statistical analysis evaluated the accuracy of the measurements obtained from each of the three sampling techniques and the intra- and interobserver reliability. *Results.* Intraobserver and interobserver reliability measures of functional data were homogeneous without statistically significant differences. Intraobserver correlation coefficients ranged from 0.94–0.99; interobserver correlation coefficients ranged from 0.97–0.99. Direct comparison of SPIDER- and RADIAL-sampled True-FISP

\*Correspondence: Jonathan S. Lewin, M.D., Department of Radiology, University Hospitals of Cleveland Case Western Reserve University, 11100 Euclid Ave., Cleveland, OH 44106-5056, USA; Fax: (216) 844-8062; E-mail: lewin@uhrad.com.

sequences showed no statistically significant differences in measured functional parameters with interstudy correlation coefficients from 0.88–0.98. RADIAL and SPIDER images had better temporal resolution and were qualitatively judged to provide superior wall/blood border definition. Statistically significant differences were identified in each volumetric functional parameter when results from the rectilinear sampling acquisitions were compared with either radial or SPIDER sampling techniques. RADIAL and SPIDER results were consistently higher than volumetric measures obtained from the rectilinear data set. *Conclusion.* Employing faster sampling schemes led to enhanced signal homogeneity while maintaining the necessary CNR for estimation of functional cardiac parameters. Enhanced signal homogeneity and maintained CNR will most likely improve the accuracy of the cardiac functional parameter determination.

*Key Words:* Cardiac MRI; Volumetric analysis; Radial; Cine true-FISP.

## INTRODUCTION

Magnetic resonance imaging (MRI) has the potential to provide high-resolution images of the heart at any point in the cardiac cycle. Its ability to provide excellent contrast between the epicardium, myocardium, and ventricular blood pool, as well sufficient spatial resolution to differentiate between papillary muscles and myocardium, establishes cardiac MR as a completely non-invasive method for visualizing ventricular structures. In particular, the end-diastolic (ED) and end-systolic (ES) left ventricular volumes, as well as derived ratios such as ejection fraction (EF) and left ventricular myocardial mass (LMM), are important indicators and predictors of heart failure that can already be measured in MR (Hammermeister et al., 1979; Utz et al., 1987).

The effort to develop sequences suitable for cardiac imaging has repeatedly come up against the fact that temporal resolution and spatial resolution are competing objectives in cardiac MRI. The introduction of both prospective and retrospective cardiac gating has offset the effects of cardiac motion and has led to gains in spatial resolution (Lanzer et al., 1984; Lenz et al., 1989). The advent of steady-state imaging with refocusing gradients along all axes during any repetition time (TR) (a.k.a., True-FISP) permits high resolution imaging at short scan times. These sequences have increased temporal resolution of cardiac MR and have exploited differences in relaxation rates between the blood pool and myocardium (Suga et al., 1999).

Rectilinear k-space sampling schemes require multiple cardiac cycles for an interleaved filling of k-space to finally reconstruct multiple images of a heart contraction. On the other hand, implementation of radial k-space acquisitions with filtered back-projection (RADIAL) and steady-state projection imaging with dynamic echo-train readout (SPIDER), allow the

acquisition of an image series in exactly one heart-beat per short-axis location utilizing a sequential filling of k-space for each image due to an accelerated, nonrectilinear and sparse sampling of k-space.

In this prospective study, we sought to compare ECG-gated rectilinear k-space sampling scheme acquired over several cardiac cycles with faster real-time radial sampling strategies, such as RADIAL and SPIDER techniques, to determine whether the inherent decrease in spatial resolution would yield a difference in measured functional cardiac parameters, while each image data set is acquired with a similar True-FISP method.

## MATERIALS AND METHODS

### Volunteers

Imaging experiments were performed under a protocol approved by the institutional review board for human investigation at our institution. After obtaining informed written consent, 10 healthy volunteers, 7 males and 3 females, underwent MR imaging. The males ranged in age from 24–40 years, mean age 32.3; the females ranged in age from 23–34 years, mean age 26.7. The volunteers had no history of cardiac disease and had normal findings at physical examinations within one year of the investigation. For all subjects, MR-compatible ECG electrodes were placed on the chest before imaging and were attached to the MR imaging unit for electrocardiographic gating.

### MR—Technique

All imaging was performed on a 1.5 T imaging system (Magnetom Sonata, Siemens, Erlangen, Germany) equipped with high-performance gradients with a

maximum amplitude of 40 mT/m and maximum slew rate of 200 mT/m/ms using a four-channel torso phased-array coil. Two long-axis and sufficient short axis breath-hold cine image series to cover the whole left ventricle were acquired with each method with the same spatial resolution of 5-mm slice thickness and 3 mm gap and the field of view kept constant for all three sampling schemes of 250–300\*300 mm. Fast imaging with steady-state precession with balanced gradients in all spatial directions (True-FISP), was utilized employing the following three k-space sampling schemes:

1. **Rectilinear** sampled **True-FISP**: TR/TE 2.96/1.58 ms; flip angle 70°; number of signal averages 1; matrix size 208\*256; in-plane spatial resolution 1.38 mm; acquisition time per cine frame and heartbeat 47.5 ms, however 15 heartbeats are necessary for complete interleaved filling of k-space; total acquisition time of 15 heartbeats, approximately 12–15 s. Prospectively cardiac gated. A linear k-space reordering scheme with Cartesian, horizontal k-space trajectories was employed. This clinically utilized sequence and k-space sampling scheme were regarded as the gold standard for

analyzing the performance of the accelerated k-space reordering schemes (Lee et al., 2002).

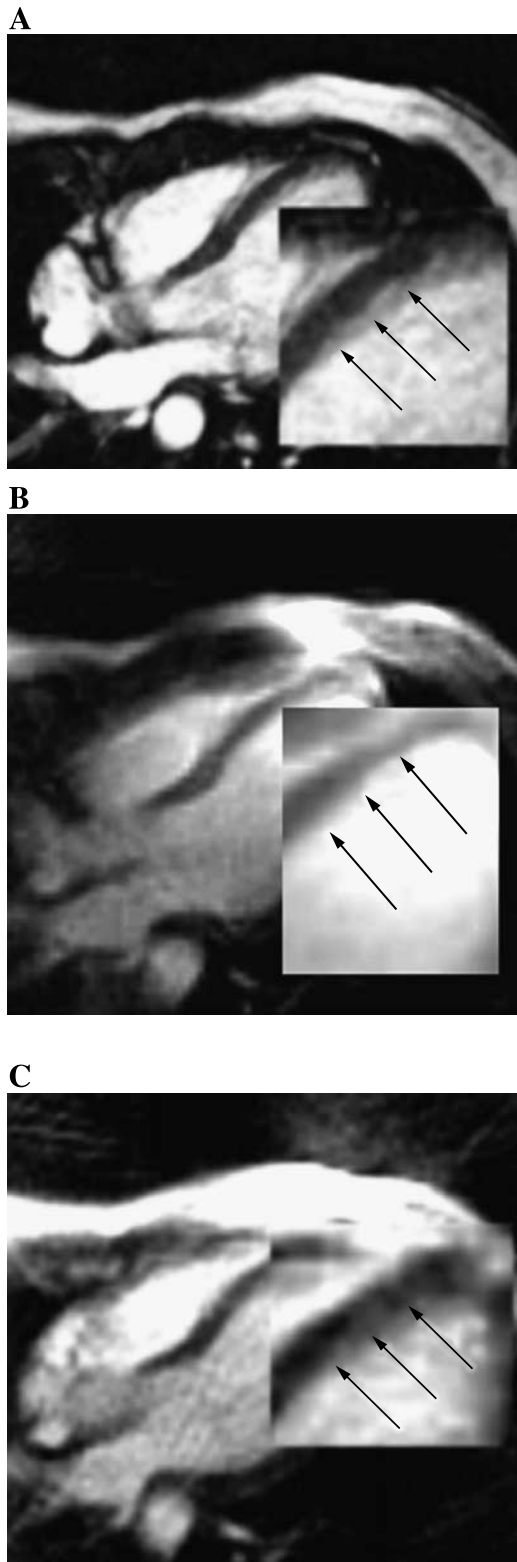
2. **Radially** sampled **True-FISP**: TR/TE 2.45/1.25 ms; flip angle 50°; number of signal averages 1; matrix size 52\*128, however, employing 50% view, sharing, thereby doubling the matrix size; in-plane spatial resolution 2.34 mm; acquisition time per sequential cine frame 82.5 ms; total acquisition time 3.3 s. No cardiac gating. Radial k-space coverage involves obtaining polar trajectories resulting in a sparse sampling of k-space (Moriguchi et al., 2000), however with inherent over-sampling of the low spatial frequencies (Shankaranarayanan et al., 2001).
3. **SPIDER** sampled **True-FISP**: TR/TE 3.39/1.62 ms; flip angle 55°; number of signal averages 1; matrix size 32\*128 utilizing 50% view sharing; in-plane spatial resolution 2.34 mm; acquisition time per sequential cine frame 90 ms; total acquisition time 1.8 s. No cardiac gating. To acquire a larger number of radial k-space samples per unit time, a single full-echo pulse plus two asymmetric echoes were recorded. In this sequence, the first and third neighboring echoes asymmetrically sampled

Table 1. Arithmetical mean±standard deviation (range).

Quantitative analysis			
Signal intensities			
	Sampling schemes		
	Rectilinear	RADIAL	SPIDER
SI <sub>Blood</sub>	395.40±36.30 (309.5–487.7)	78.07±6.32 (64.6–91.9)	154.67±9.16 (135.5–172.5)
SI <sub>Myocardium</sub>	87.64±21.65 (53.4–131.9)	27.66±5.19 (21.4–36.2)	54.12±7.93 (46.6–70.1)
SI <sub>Noise</sub>	65.08±13.36 (23.2–92.1)	15.92±4.58 (6.7–26.4)	20.63±5.54 (9.97–34.1)
SNR <sub>Blood</sub>	29.06±3.12 (15.0–55.1)	17.01±2.58 (7.4–31.4)	27.88±5.64 (9.3–5.6)
SNR <sub>Myocardium</sub>	6.58±1.33 (1.5–16.9)	6.04±2.24 (1.2–14.4)	9.77±3.54 (1.9–31.6)
CNR <sub>Blood/Myocardium</sub>	22.34±3.91 (16.2–29.3)	10.55±2.08 (8.0–14.6)	17.01±5.76 (8.25–27.95)
Statistical analysis of signal intensities			
	Sampling schemes		
	Rectilinear vs. RADIAL	Rectilinear vs. SPIDER	RADIAL vs. SPIDER
SNR <sub>Blood</sub>	<0.001*	0.2802	<0.001*
SNR <sub>Myocardium</sub>	0.3933	0.001*	0.002*
CNR <sub>Blood/Myocardium</sub>	<0.001*	0.0500	<0.001*

Abbreviations: SI—signal intensities; SNR—signal-to-noise ratios; CNR—contrast-to-noise ratios.

\*Student’s T-test detected statistically significant differences (p<.05).



69 of 128 readout points, whereas the second echo sampled all 128 readout points (Larson and Simonetti, 2001).

### Quantitative Analysis

The background signal intensity, as well as the signal intensities of intraventricular blood pool and septal, apical, and lateral myocardium were measured on corresponding long-axis data sets in all frames in a cardiac cycle. Regions of interest (ROIs) were placed on homogeneous structures in artifact-free zones. ROIs for background signal intensity included at least 500 pixels and were placed anterior to the chest wall; ROIs for blood and septal, apical, and lateral myocardium intensities included at least 20 pixels. For the intensity measurements on each frame, three separate ROIs from different areas were evaluated and the results averaged. Mean background noise was measured for each frame along the phase-encoding axis for rectilinearly sampled images, and in areas of no inherent signal for radial and SPIDER schemes. For all image data sets, the  $\text{signal}_{\text{blood}}$ -to-noise ratios were calculated following the standard formula:

$$\text{SNR}_{\text{blood}} = \text{SI}_{\text{blood}} / \text{SD}_{\text{noise}}$$

Accordingly, the  $\text{signal}_{\text{myocardium}}$ -to-noise ratios were evaluated:

$$\text{SNR}_{\text{myocardium}} = \text{SI}_{\text{myocardium}} / \text{SD}_{\text{noise}}$$

The blood–myocardial contrast-to-noise ratios were computed as

$$\text{CNR} = (\text{SI}_{\text{blood}} - \text{SI}_{\text{myocardium}}) / \text{SD}_{\text{Noise}}$$

**Figure 1.** Horizontal long-axis MR images in a healthy volunteer. True-FISP cine imaging during ED phase. (A) Rectilinear k-space sampling of multiple cardiac gated heartbeats showed the highest signal intensity for blood and myocardium as well as contrast-to-noise ratio. Note the motion artifacts in the septal and apical myocardial portion (arrows in magnified inset). (B) The SPIDER sampling scheme presented blood intensity values without significant differences when compared to the rectilinear sampling scheme; however, there was an increase in noise. Note the well-demarcated myocardial structures imaged during one heartbeat (arrows in magnified inset) are distinct enough for precise automatic segmentation of endocardial and pericardial interfaces. (C) The RADIAL-sampled True-FISP sequence demonstrated a relative loss of signal intensity in the blood pool with an additional increase of noise when compared to either rectilinear or SPIDER sampled sequences. The myocardium, however, is presented sufficiently well demarcated (arrows in magnified inset) for successful automatic segmentation of endocardium and pericardium.

**Table 2.** Mean standard deviation of observed intraobserver differences with associated 95% confidence interval (CI).

	Functional analysis—intraobserver reliability		
	Sampling schemes		
	Rectilinear	RADIAL	SPIDER
<b>ED</b> left ventricular volume	<b>1.18 ml</b> (CI 0.87–1.49 ml)	<b>1.30 ml</b> (CI 0.89–1.72 ml)	<b>1.06 ml</b> (CI 0.76–1.36 ml)
<b>ES</b> left ventricular volume	<b>1.07 ml</b> (CI 0.83–1.32 ml)	<b>1.01 ml</b> (CI 0.75–1.27 ml)	<b>1.03 ml</b> (CI 0.59–1.47 ml)
Left ventricular <b>Mass</b>	<b>1.28 g</b> (CI 0.90–1.66 g)	<b>1.83 g</b> (CI 1.11–2.45 g)	<b>1.25 g</b> (CI 0.87–1.63 g)
Left ventricular <b>EF</b>	<b>1.33%</b> (CI 1.00–1.66%)	<b>1.04%</b> (CI 0.63–1.44%)	<b>0.87%</b> (CI 0.57–1.17%)

No statistical significant intraobserver differences during measurement repetitions were detected for any observer ( $p > 0.05$ ).

*Abbreviations:* ED—end-diastolic; ES—end-systolic; EF—ejection fraction.

A Student's T-Test was utilized to determine statistically significant differences. Statistical analysis was performed using SPSS V11.0 (SPSS, Chicago, IL, USA). A  $p$  value of less than 0.05 was considered to be statistically significant.

### Functional Analysis

The semiautomatic functional image analysis was performed by two independent investigators three times for each volunteer and for each sampling technique, with an interval of more than a week between each measurement repetition. The definition of left ventricular endocardium and pericardium were realized by manually marking the ventricular lumen and the myocardial wall, respectively. Subsequently, automated segmentation techniques detected endocardial as well as pericardial interfaces. The calculation of three-dimensional (3D) volumes based on those segmented two-dimensional (2D) areas on short-axis imaging planes, which ranged from the cardiac base to the apex, was realized by algorithms for automatic geometrical assumptions. In this way, left ventricular volumes and LMM as well as EF were calculated, utilizing commercially available software (Argus, Siemens, Erlangen, Germany). The

most basal ventricular image series was defined as the section in which the left ventricular myocardium extended over at least 50% of the circumference of the left ventricular chamber. Endocardial and pericardial contours were drawn on all ED and ES frame data sets. Papillary muscles were included in the left ventricular volume.

Interstudy as well as inter- and intraobserver reliabilities were determined for the parameters “ED left ventricular volume,” “ES left ventricular volume,” “LMM,” and “EF” utilizing the Bartko-Carpenter approach (Bartko and Carpenter, 1976) as well as by calculating the standard deviation of the observed differences with associated 95% confidence interval for inter- and intraobserver analysis. Intraobserver reliability was analyzed by computing the analysis of variance (ANOVA) intraclass correlation coefficient,  $\kappa_{\text{intra class}}$ , for each reader on each data subset of the three sampling schemes. Interobserver reliability was calculated utilizing the ANOVA interclass coefficient,  $\kappa_{\text{inter class}}$ , for both readers on the mean of each data subset for each of the three sampling techniques. Interstudy reliability was determined by analysis of the ANOVA interstudy correlation coefficient,  $\kappa_{\text{inter study}}$ , for both readers on every subset of all possibly comparable

**Table 3.** Mean standard deviation of observed interobserver differences with associated 95% confidence interval (CI).

	Functional analysis—interobserver reliability		
	Sampling schemes		
	Rectilinear	RADIAL	SPIDER
<b>ED</b> left ventricular volume	<b>2.85 ml</b> (CI 1.08–4.61 ml)	<b>2.62 ml</b> (CI 1.00–4.25 ml)	<b>1.86 ml</b> (CI 0.71–3.01 ml)
<b>ES</b> left ventricular volume	<b>1.76 ml</b> (CI 0.67–2.85 ml)	<b>1.38 ml</b> (CI 0.52–2.23 ml)	<b>0.96 ml</b> (CI 0.37–1.56 ml)
Left ventricular <b>Mass</b>	<b>1.85 g</b> (CI 0.70–2.99 g)	<b>2.09 g</b> (CI 0.80–3.39 g)	<b>2.06 g</b> (CI 0.78–3.34 g)
Left ventricular <b>EF</b>	<b>1.10%</b> (CI 0.42–1.78%)	<b>0.98%</b> (CI 0.37–1.59%)	<b>0.73%</b> (CI 0.28–1.18%)

No statistical significant interobserver differences between observers were detected ( $p > 0.05$ ).

pairs of the three k-space sampling modalities and additionally mean differences with corresponding standard deviations were calculated.

A Student's T-Test was utilized to determine statistically significant differences in intraobserver and interobserver datasets as well as interstudy data pairs. The T-Tests evaluated the intraobserver standard deviations of observed differences of the repetitive measurements and compared all possible pairs of the three k-space sampling methods. Furthermore, interobserver and interstudy differences of ED and ES volumes as well as LMM and EF were analyzed. A *p*-value of less than 0.05 was considered to be statistically significant. To realize this significance level in a statistical analysis consisting of multiple independent significant tests, Bonferroni correction was employed. Individual *p*-values of less than 0.017 guaranteed an overall corrected *p*-value of less than 0.05.

## RESULTS

### Quantitative Analysis

The signal intensities (SI) as well as signal to noise ratios (SNR) for the ventricular blood pool and septal,

apical, and lateral myocardium as well as corresponding contrast to noise ratio (CNR) acquired with cine True-FISP sequences employing rectilinear, RADIAL, and SPIDER k-space sampling are listed in Table 1. The quantitative analysis demonstrated that the SNR values for blood and the overall CNR values for blood and myocardium of the SPIDER k-space acquisition scheme did not show statistically significant differences compared to the rectilinear k-space technique. Whereas RADIAL k-space coverage showed statistically significant lower SNR values for the ventricular blood pool as well as lower CNR values for blood and myocardium when compared to both rectilinear and SPIDER k-space sampling methods (Fig. 1).

### Functional Analysis

The *intraobserver reliability* presented homogeneous intraobserver patterns with intraobserver kappa values ranging from  $\kappa_{\text{intraclass}}$  0.94 to 0.99 for the analyzed parameters "ED left ventricular volume," "ES left ventricular volume," as well as the derived parameter "LMM." However, the derived parameter "EF" presented decreased intraobserver kappa values ranging from  $\kappa_{\text{intraclass}}$  0.60–0.63 for the rectilinear sampled sequence in contrast to kappa values of

**Table 4.** The interstudy comparison as well as student's *t* test presented statistically significant degrees of data inhomogeneity [indicated by † and \*, respectively] when rectilinear sampled data sets are compared either to RADIAL- or SPIDER-sampling schemes, whereas a direct comparison of the latter two sampling schemes resulted in homogeneous data sets.

	Functional analysis—interstudy evaluation		
	Sampling schemes		
	Rectilinear vs. RADIAL	Rectilinear vs. SPIDER	RADIAL vs. SPIDER
<i>K<sub>Interstudy</sub> Values</i>			
ED left ventricular volume	<b>0.79</b> †	<b>0.76</b> †	0.96
ES left ventricular volume	<b>0.60</b> †	<b>0.37</b> †	0.88
Left ventricular <b>Mass</b>	0.96	0.96	0.98
Left ventricular <b>EF</b>	<b>0.71</b> †	<b>0.62</b> †	0.81
<i>Mean differences ± SD</i>			
ED left ventricular volume	<b>27.41</b> ± 14.3 ml	<b>28.36</b> ± 14.5 ml	4.7 ± 4.1 ml
ES left ventricular volume	<b>12.45</b> ± 8.3 ml	<b>12.47</b> ± 9.8 ml	4.2 ± 3.1 ml
Left ventricular <b>Mass</b>	7.99 ± 5.6 g	6.13 ± 5.6 g	3.78 ± 2.7 g
Left ventricular <b>EF</b>	4.2 ± 3.9%	5.4 ± 4.7%	2.7 ± 2.1%
<i>Statistical analysis; t test</i>			
ED left ventricular volume	< <b>0.001</b> *	< <b>0.001</b> *	0.41
ES left ventricular volume	< <b>0.001</b> *	< <b>0.001</b> *	0.48
Left ventricular <b>Mass</b>	0.09	0.13	0.27
Left ventricular <b>EF</b>	0.35	0.29	0.8

In all cases, ventricular volume as well as EF and LMM results from RADIAL- and SPIDER-sampled acquisitions were consistently higher than those obtained from the rectilinear acquisitions.

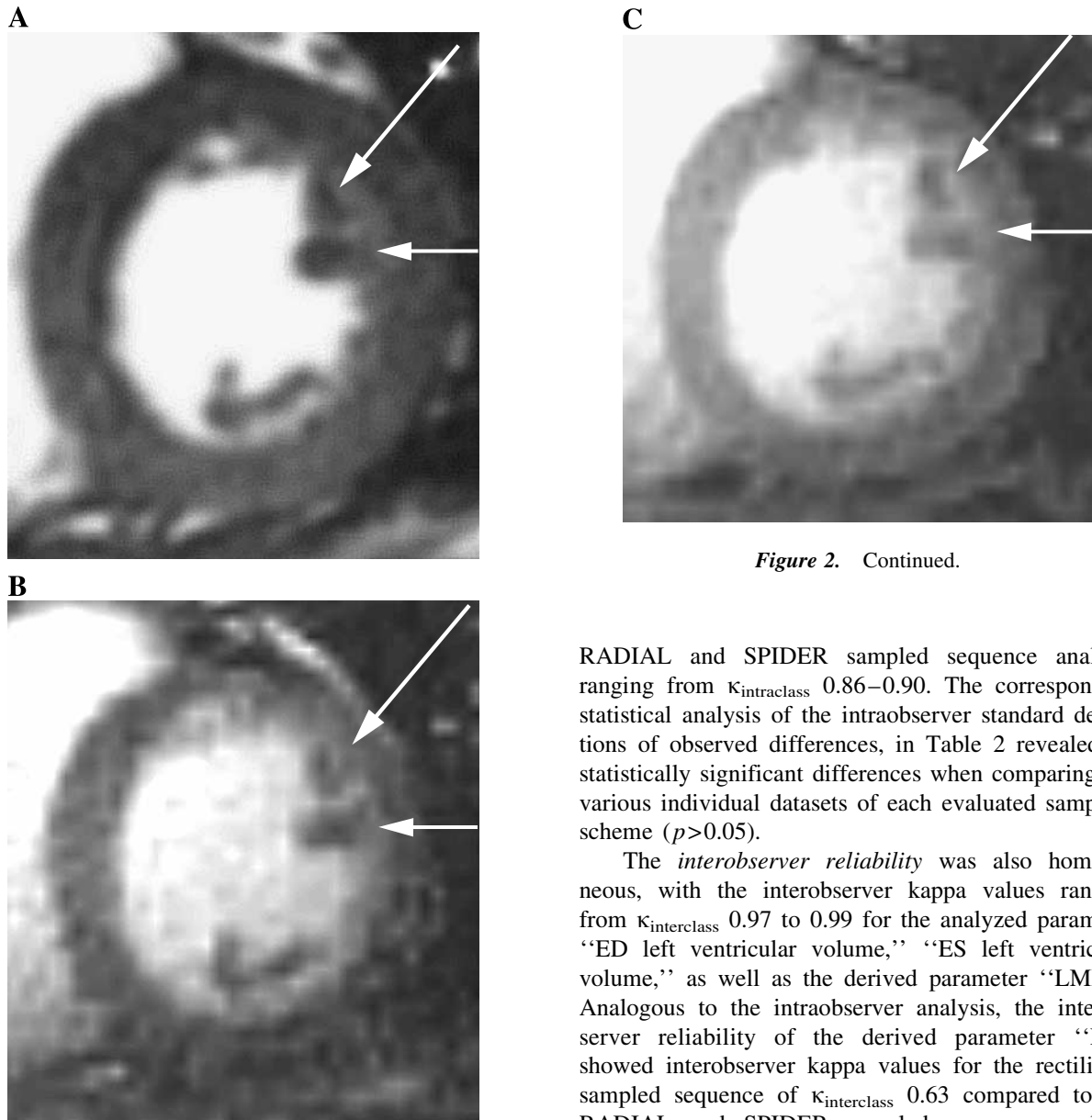


**Figure 2.** Midventricular short-axis MR images in a healthy volunteer. True FISP cine imaging during ED phase. (A) Rectilinear k-space sampling did not demonstrate a clear separation between the myocardial wall and the papillary muscles (arrows) and therefore differentiation by means of automatic segmentation was not successful. (B) The SPIDER-sampling scheme and (C) RADIAL-sampled True-FISP sequence allowed a differentiation between papillary muscle and ventricular myocardium (arrows) by means of automatic segmentation.

**Figure 2.** Continued.

RADIAL and SPIDER sampled sequence analysis ranging from  $\kappa_{\text{intraobserver}}$  0.86–0.90. The corresponding statistical analysis of the intraobserver standard deviations of observed differences, in Table 2 revealed no statistically significant differences when comparing the various individual datasets of each evaluated sampling scheme ( $p > 0.05$ ).

The *interobserver reliability* was also homogeneous, with the interobserver kappa values ranging from  $\kappa_{\text{interobserver}}$  0.97 to 0.99 for the analyzed parameter “ED left ventricular volume,” “ES left ventricular volume,” as well as the derived parameter “LMM.” Analogous to the intraobserver analysis, the interobserver reliability of the derived parameter “EF” showed interobserver kappa values for the rectilinear sampled sequence of  $\kappa_{\text{interobserver}}$  0.63 compared to the RADIAL and SPIDER sampled sequence analysis ranging from  $\kappa_{\text{interobserver}}$  0.88–0.91. The interobserver standard deviations of observed differences in Table 3 revealed no statistically significant differences when comparing the datasets analyzed by each observer evaluating various sampling schemes ( $p > 0.05$ ).

The *interstudy reliability* analysis, presented as a direct comparison of RADIAL sampled and SPIDER sampled cine True-FISP sequences, revealed significantly homogeneous datasets without statistically significant differences for “ED left ventricular volume” and “ES left ventricular volume.” This direct comparison further highlighted significant data homogeneity and no statistically significant differences when analyzing “LMM” and “EF” (Table 4).

The statistical analysis was able to prove a significant degree of data inhomogeneity and statistical difference when comparing the interstudy reliability of the rectilinear sampled and the RADIAL sampled cine True-FISP sequences estimate of "ED left ventricular volume" and "ES left ventricular volume" (Table 4). In all cases, ventricular volume results from rectilinearly sampled acquisitions were consistently less than those obtained with RADIAL acquisitions caused by a pronounced segmentation mismatch of apical cardiac structures. Comparing rectilinear sampled with RADIAL sampled cine True-FISP sequences, data inhomogeneity and variations were less evident when the derived parameters "LMM" and "EF" were analyzed (see Table 4 for evaluation of data inhomogeneity and statistical analysis of the data variations) (Fig. 2).

The evaluation of the interstudy reliability comparing the rectilinear sampled cine True-FISP sequence with the SPIDER sampled sequence, also revealed significant data inhomogeneity as well as statistically significant differences for the analyzed parameters "ED left ventricular volume" and "ES left ventricular volume." Analogously, the ventricular volume results from rectilinearly sampled acquisitions were consistently less than those obtained with SPIDER acquisitions, showing an analogous segmentation mismatch of apical cardiac structures. Again, data inhomogeneity and variations were less evident when analysis was focusing on the derived parameters "LMM" and "EF" (see Table 4 for evaluation of data inhomogeneity and statistical analysis of data variations) (Fig. 2).

## DISCUSSION

Over the past decade, cardiac MR imaging has evolved as a visualization technique, allowing reliable imaging of cardiac morphology as well as analysis of cardiac function by calculation of cardiac volumes. In MR imaging, temporal and spatial resolution are competing objectives. Therefore, cardiac MRI presents the challenge of developing sequences that meet the requirement for high resolution images that differentiate the complex anatomy of the heart, while also being fast enough to offset the effects of nonrigid cardiac motion.

In particular, left ventricular ED and ES volumes represent important parameters in the management of cardiac diseases (Koneremann et al., 1992). These parameters function as predictors of mortality and progression of acute as well as chronic heart failure (Hammermeister et al., 1979). Variability and repro-

ducibility are critical parameters for any functional imaging for modality of the heart. Improving the accuracy of cardiac MR imaging techniques allows cardiac MR to be used more interchangeably with other complementary modalities in the course of managing cardiac diseases (Darasz et al., 2002; Heusch et al., 1999; Mogelvang et al., 1992).

The use of True-FISP cine sequences leads to fast imaging of the cardiac morphology at high spatial resolution, and, further, allows analysis of cardiac function. However, rectilinear k-space sampling schemes utilize ECG-gated data sets of multiple cardiac cycles to reconstruct and visualize one averaged contraction of the heart. Therefore, calculations of the cardiac volumes are based on spatial data averaged over multiple heart cycles. In this prospective study, we evaluated whether utilizing real-time sampling schemes, such as RADIAL and SPIDER techniques, would yield differences in measured left ventricular volumes when compared to those obtained with rectilinear sampling.

This study was able to prove that faster sampling schemes, such as RADIAL and SPIDER, lead to a significant increase in data homogeneity compared to the rectilinear sampling technique. This can be seen from the analysis of ED and ES left ventricular volumes as well as EF and LMM. This study demonstrated that ED and ES left ventricular volumes defined on RADIAL and SPIDER sampled datasets, present statistically significant differences compared to the rectilinear sampled image series. No significant differences are identified when RADIAL and SPIDER sampled techniques are statistically evaluated against each other.

The automated segmentation without manual correction of the left myocardial structures based on rectilinear sampled data sets showed apparent weaknesses in identifying apical ventricular structures, in particular, rectilinear data sets suffered in defining apical papillary muscles, as well as in differentiating between apical myocardium and pericardial and diaphragmal structures. Those effects were most evident when considering absolute ventricular volumes. However, as long as the clinically proven rectilinear sampling scheme of a True-FISP sequence is considered the internal gold standard, this study proved that faster sampling schemes with inherent decrease of spatial resolution, such as RADIAL and SPIDER, lead to significantly larger ED and ES left ventricular volumes compared to rectilinear sampling.

Intraobserver and interobserver analysis focusing on the degree of data reliability presented homogeneous data sets for all analyzed parameters in concordance with previously performed studies (Forbat et al., 1996).

This study furthermore revealed that the contrast-to-noise ratio achieved by the SPIDER sampling technique showed no statistically significant intensity difference when compared to those found with the rectilinear sampling scheme. The analysis of the signal-to-noise ratio of the blood pool and myocardium was not able to demonstrate significant difference in the blood intensity of SPIDER-sampled sequences compared to the rectilinear sampling scheme; however, a statistically significant difference in myocardial intensity was observed. On the other hand, the RADIAL-sampled sequences revealed a statistically significant difference for blood pool intensity and subsequent contrast-to-noise intensity when compared to the rectilinear sampling scheme caused by an intensity loss in the blood pool due to inflow artifacts (Shankaranarayanan et al., 2001).

Although this study was performed with a small group of young and healthy volunteers, and did not include patients with cardiac disease, the significant differences in the functional parameters are evident when faster sampling schemes allow visualization of one actual cardiac contraction per short-axis location. Patients with cardiac disease will appreciate the acquisition time reduction even more because of shorter breath-hold periods required. Another limitation of our study design was the absence of an external gold standard, which usually utilizes more invasive imaging modalities with the additional use of ionizing radiation. Instead, we employed the clinically utilized rectilinear sampled True-FISP sequence as the internal reference standard.

Furthermore, the influence of new real-time radial acquisition schemes on characteristic visualization of blood pool and myocardial wall have not yet been evaluated in specific studies. It can be hypothesized, however, that not only spatial and temporal resolutions of real-time radial acquisition schemes but also inherent excitation effects influenced the obtained measurement differences.

Those fast-sampling schemes evaluated allow visualization of only one actual cardiac contraction per short-axis location and had to be repeated for coverage of the entire left ventricle. It can be hypothesized that future studies analyzing thin slice and high resolution visualization of the left ventricle in various short axes series simultaneously during one actual cardiac contraction will present further improvement in functional accuracy.

We therefore conclude that employing faster sampling schemes with an inherent decrease of spatial resolution leads to enhanced signal homogeneity and will therefore improve anatomical border definition

while maintaining the necessary CNR to estimate functional cardiac parameters. Enhanced signal homogeneity and maintained CNR will most likely improve the accuracy of the cardiac functional parameter determination.

## REFERENCES

- Bartko, J. J., Carpenter, W. T., Jr. (1976). On the methods and theory of reliability. *J. of Nerv. Ment. Dis.* 163:307–317.
- Darasz, K. H., Underwood, S. R., Bayliss, J., Forbat, S. M., Keegan, J., Poole-Wilson, P. A., et al. (2002). Measurement of left ventricular volume after anterior myocardial infarction: comparison of magnetic resonance imaging, echocardiography, and radionuclide ventriculography. *Int. J. Cardiovasc. Imag.* 18:135–142.
- Forbat, S. M., Sakrana, M. A., Darasz, K. H., El Demerdash, F., Underwood, S. R. (1996). Rapid assessment of left ventricular volume by short axis cine MRI. *Br. J. Radiol.* 69:221–225.
- Hammermeister, K. E., DeRouen, T. A., Dodge, H. T. (1979). Variables predictive of survival in patients with coronary disease. Selection by univariate and multivariate analyses from the clinical, electrocardiographic, exercise, arteriographic, and quantitative angiographic evaluations. *Circulation* 59: 421–430.
- Heusch, A., Koch, J. A., Krogmann, O. N., Korbmacher, B., Bourgeois, M. (1999). Volumetric analysis of the right and left ventricle in a porcine heart model: comparison of three-dimensional echocardiography, magnetic resonance imaging and angiocardiology. *Eur. J. Ultrasound* 9:245–255.
- Konermann, M., Grotz, J., Altmann, C., Laschewski, F., Josephs, W., Hotzinger, H. (1992). Left ventricular dimensions and functions in the acute and chronic phase after myocardial infarct—comparison of cine-magnetic resonance tomography, angiocardiology, 2D-echocardiography and technetium ventricular scintigraphy. *Z. Kardiol.* 81: 610–618.
- Lanzer, P., Botvinick, E. H., Schiller, N. B., Crooks, L. E., Arakawa, M., Kaufman, L., et al. (1984). Cardiac imaging using gated magnetic resonance. *Radiology* 150:121–127.
- Larson, A. C., Simonetti, O. P. (2001). Real-time cardiac cine imaging with SPIDER: steady-state projection imaging with dynamic echo-train readout. *Magn. Reson. Med.* 46:1059–1066.
- Lee, V. S., Resnick, D., Bundy, J. M., Simonetti, O. P.,

- Lee, P., Weinreb, J. C. (2002). Cardiac function: MR evaluation in one breath hold with real-time true fast imaging with steady-state precession. *Radiology* 222:835–842.
- Lenz, G. W., Haacke, E. M., White, R. D. (1989). Retrospective cardiac gating: a review of technical aspects and future directions. *Magn. Reson. Imaging* 7:445–455.
- Mogelvang, J., Stokholm, K. H., Saunamaki, K., Reimer, A., Stubgaard, M., Thomsen, C., et al. (1992). Assessment of left ventricular volumes by magnetic resonance in comparison with radionuclide angiography, contrast angiography and echocardiography. *Eur. Heart J.* 13:1677–1683.
- Moriguchi, H., Wendt, M., Duerk, J. L. (2000). Applying the uniform resampling (URS) algorithm to a lissajous trajectory: fast image reconstruction with optimal gridding. *Magn. Reson. Med.* 44:766–781.
- Shankaranarayanan, A., Wendt, M., Lewin, J. S., Duerk, J. L. (2001). Two-step navigatorless correction algorithm for radial k-space MRI acquisitions. *Magn. Reson. Med.* 45:277–288.
- Suga, M., Matsuda, T., Komori, M., Minato, K., Takahashi, T. (1999). Keyhole method for high-speed human cardiac cine MR imaging. *J. Magn. Reson. Imaging* 10:778–783.
- Utz, J. A., Herfkens, R. J., Heinsimer, J. A., Bashore, T., Califf, R., Glover, G., et al. (1987). Cine MR determination of left ventricular ejection fraction. *AJR Am. J. Roentgenol.* 148:839–843.

Submitted February 12, 2003

Accepted March 22, 2004